Chinese Journal of Aeronautics, (2013),26(5): 1251–1258

Chinese Society of Aeronautics and Astronautics
& Beihang University

Chinese Journal of Aeronautics

cja@buaa.edu.cn
www.sciencedirect.com

# $H_\infty$ output tracking control for flight control systems with time-varying delay

**Zhang Yingxin** [a], **Wang Qing** [a,*], **Dong Chaoyang** [b], **Jiang Yifan** [a]

[a] *School of Automation Science and Electrical Engineering, Beihang University, Beijing 100191, China*
[b] *School of Aeronautic Science and Engineering, Beihang University, Beijing 100191, China*

Received 23 July 2012; revised 17 September 2012; accepted 7 January 2013
Available online 31 July 2013

**KEYWORDS**

Discrete time control systems;
Flight control systems;
$H_\infty$ output tracking;
Time-varying delay;
Uncertainty

**Abstract** For flight control systems with time-varying delay, an $H_\infty$ output tracking controller is proposed. The controller is designed for the discrete-time state-space model of general aircraft to reduce the effects of uncertainties of the mathematical model, external disturbances, and bounded time-varying delay. It is assumed that the feedback-control loop is closed by the communication network, and the network-based control architecture induces time-delays in the feedback information. Suppose that the time delay has both an upper bound and a lower bound. By using the Lyapunov-Krasovskii function and the linear matrix inequality (LMI), the delay-dependent stability criterion is derived for the time-delay system. Based on the criterion, a state-feedback $H_\infty$ output tracking controller for systems with norm-bounded uncertainties and time-varying delay is presented. The control scheme is applied to the high incidence research model (HIRM), which shows the effectiveness of the proposed approach.



## 1. Introduction

In the traditional communication architecture for flight control systems, internal sensors and actuators are connected to controllers by wires. For cases that sensors are located in different places, the feedback-control loop is closed via a shared communication network,[1] for example, flight information is obtained by satellite or ground-based radar. The usage of a shared network offers the benefit of increased flexibility of the system architecture.[2] On the other hand, the data latency of messages in the shared network induces time delay in the network-based control system. For flight control systems, time delay can influence flying quality and reliability of aircraft, which requires much effort to remedy.[3,4]

Stability analysis is the foundation of research on time-delay systems. From Ref. [5] it is known that a network-based flight control system with delayed communication can be modeled as an interval time-varying delay system. Most of the existing delay-dependent stability criteria are obtained by using the Lyapunov-Krasovskii approach or the Lyapunov-Razumikhin approach.[6] For continuous-time systems, researchers have introduced various Lyapunov functions and corresponding stability criteria are obtained. For discrete-time systems, fewer efforts have been made and there still leaves much room for improvement.

* Corresponding author. Tel.: +86 10 82338161.
E-mail addresses: zyxbuaa@gmail.com (Y. Zhang), wangqing@buaa.edu.cn (Q. Wang).

Peer review under responsibility of Editorial Committe of CJA.

ELSEVIER Production and hosting by Elsevier


http://dx.doi.org/10.1016/j.cja.2013.07.024

It is known that in engineering systems, dynamics cannot be modeled with absolute precision[7] and parameter uncertainties are frequently encountered.[8] Over the past decade, the robust tracking and model following problem for dynamic systems with uncertainties has been widely investigated.[9] In Ref. [10] the effects of uncertainties of aerodynamic parameters on robustness were investigated. Bresch-Pietri and Krstic[11] designed an adaptive trajectory tracking controller for an ordinary differential equation (ODE) system with unknown input delay and parameters.

Considering the network-based flight control systems, the authors analyzed stability of full-envelope network-based flight control systems[2] and robust trajectory tracking control of aircraft with time-varying delay.[12] For actual flight control systems with a shared communication network, time delay and parameter uncertainties should be taken into account.

This paper presents an $H_\infty$ output tracking controller for network-based flight control systems with time delay and norm-bounded parameter uncertainties. The time delay is assumed to vary in a known range. The Lyapunov-Krasovskii function is used to establish the delay-dependent criterion. The criterion is expressed in the form of linear matrix inequalities (LMIs). According to the delay-dependent criterion, the $H_\infty$ output tracking controller is solved. The control scheme is applied to a high incidence research model (HIRM) aircraft.

## 2. Problem formulation

### 2.1. Model description

Suppose a general aircraft represented by the following dynamic equations of motion:

$$\begin{cases} \dot{V} = \dfrac{F_{wx}}{m} g \sin\gamma \\ \dot{\alpha} = q_b - \dfrac{q_w}{\cos\beta} - p_b\cos\alpha\tan\beta - r_b\sin\alpha\tan\beta \\ \dot{\beta} = r_w + p_b\sin\alpha - r_b\cos\alpha \\ \dot{\gamma} = q_w\cos\varphi - \gamma_w\sin\varphi \\ \dot{\varphi} = p_w + (q_w\sin\varphi + r_w\cos\varphi)\tan\gamma \\ \dot{\psi} = \dfrac{q_w\sin\varphi + r_w\cos\varphi}{\cos\gamma} \\ \dot{q}_b = \frac{1}{I_y}\left[M_b + I_{xz}(r_b^2 - p_b^2) + (I_z - I_x)r_b p_b\right] \\ \begin{bmatrix} \dot{p}_b \\ \dot{r}_b \end{bmatrix} = \begin{bmatrix} I_x & -I_{xz} \\ -I_{xz} & I_z \end{bmatrix}^{-1} \begin{bmatrix} L_b + I_{xz}p_b q_b + (I_y - I_z)q_b r_b \\ N_b - I_{xz}q_b r_b + (I_x - I_y)p_b q_b \end{bmatrix} \end{cases} \tag{1}$$

where $V$ denotes the flight path velocity; $\alpha$ and $\beta$ are the angle of attack and angle of sideslip, respectively; $\gamma$, $\varphi$, and $\psi$ denote the wind-axis Euler angles; $p_b$, $q_b$, and $r_b$ are the body-axis angular rates; $p_w$, $q_w$, and $r_w$ are the wind-axis angular rates; $m$ denotes the mass; $F_{wx}$ is the wind-axis total force about $x$-body axis; $g$ denotes the gravity acceleration; $L_b$, $M_b$, and $N_b$ denote the body-axis total rolling, pitching, and yawing moments, respectively; $I_x$, $I_y$, and $I_z$ are the moments of inertia about $x$-, $y$-, and $z$-body axes; $I_{xz}$ denotes the cross product of inertia with respect to $x$- and $z$-body axes. The transformations between the various axial systems used in the mathematical model (1) are standard.

For design purpose, it is supposed that the aircraft is in a wings-level steady-state flight condition. In this case, the roll angle is zero. If the sideslip angle is negligible and the roll and yaw rates are low, the six-DOF equations of motion can be translated into a pure longitudinal motion.

Suppose the flight path velocity is constant. By linearization on the equilibrium point, the longitudinal state-space model decoupled from Eq. (1) is given as follows:

$$\dot{\boldsymbol{x}}(t) = \boldsymbol{A}_p\boldsymbol{x}(t) + \boldsymbol{B}_p\boldsymbol{u}(t) + \boldsymbol{E}_p\boldsymbol{w}(t) \tag{2}$$

where $\boldsymbol{x}(t) = [\alpha \quad q_b \quad \theta]^T$ is the longitudinal motion state vector, $\theta$ the pitch angle, $\boldsymbol{u}(t)$ the elevator deflection, $\boldsymbol{w}(t)$ the external disturbance; $\boldsymbol{E}_p$ shows how the disturbance adds to the system; $\boldsymbol{A}_p$ and $\boldsymbol{B}_p$ are system matrices in the following forms:

$$\boldsymbol{A}_p = \begin{bmatrix} Z_\alpha & 1 & -g\sin(\mu_*/V_*) \\ M_\alpha & M_q & 0 \\ 0 & 1 & 0 \end{bmatrix}, \boldsymbol{B}_p = \begin{bmatrix} Z_{\delta_z} \\ M_{\delta_z} \\ 0 \end{bmatrix} \tag{3}$$

where the parameters $Z_\alpha$, $M_\alpha$, $M_q$, $Z_{\delta_z}$, and $M_{\delta_z}$ are the force and moment dimensional derivatives defined in Ref. [13], the subscript $\delta_z$ denotes the equivalent elevator deflection; $\mu_*$ and $V_*$ represent the flight-path angle and the velocity on the equilibrium point, respectively.

For other cases, the equations of motion can also be described separately as the longitudinal and later-directional parts.

### 2.2. Modeling of network-based flight control system

A typical continuous-time flight control system is given in Eq. (2). To design a discrete-time controller, the continuous-time system is discretized as follows:

$$\begin{cases} \boldsymbol{x}(k+1) = \boldsymbol{A}\boldsymbol{x}(k) + \boldsymbol{B}\boldsymbol{u}(k) + \boldsymbol{E}\boldsymbol{w}(k) \\ \boldsymbol{y}(k) = \boldsymbol{C}\boldsymbol{x}(k) + \boldsymbol{D}\boldsymbol{u}(k) \end{cases} \tag{4}$$

where $k$ is discrete time, $\boldsymbol{x}(k) \in \mathbf{R}^n$ the state vector, $\boldsymbol{u}(k) \in \mathbf{R}^p$ the control input, $\boldsymbol{y}(k) \in \mathbf{R}^q$ the output, and $\boldsymbol{w}(k) \in \mathbf{R}^l$ the disturbance that satisfies $\{\boldsymbol{w}(k)\} \in L_2[0,\infty)$; $\boldsymbol{A}$, $\boldsymbol{B}$, $\boldsymbol{C}$, $\boldsymbol{D}$, and $\boldsymbol{E}$ are appropriately dimensioned system matrices and $\boldsymbol{A} = e^{\boldsymbol{A}_p T_s}$, $\boldsymbol{B} = \int_0^{T_s} e^{\boldsymbol{A}_p t}\boldsymbol{B}_p dt$, $\boldsymbol{E} = \int_0^{T_s} e^{\boldsymbol{A}_p t}\boldsymbol{E}_p dt$, $T_s$ is the sampling time.

Fig. 1 shows the structure of a typical network-based flight control system. The insertion of the communication network in the feedback-control loop adds delays to the flight control system.[2] There are two kinds of delays according to the sources: the sensor-to-controller delay $d_{sc}(k)$ and the controller-to-actuator delay $d_{ca}(k)$. For analysis purpose, the total delay at each sampling period is denoted by $d(k) = d_{sc}(k) + d_{ca}(k)$. Therefore, it is rational to suppose that the signal $\boldsymbol{x}(k)$, which is successfully transmitted from the sensor to the controller at time $k$, has experienced signal transmission delay $d(k)$. Then the state-feedback is $\boldsymbol{x}(k - d(k))$.

Assumptions on $d(k)$ can be made as follows.

**Assumption 1.** The time delay $d(k)$ is mainly induced by the packet dropouts and is not less than a sample period.

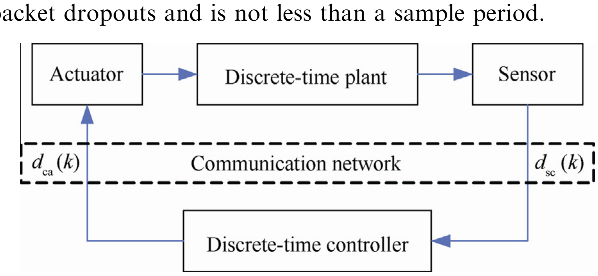


**Fig. 1** Structure of a network-based flight control system.

**Assumption 2.** The time delay $d(k)$ is assumed to be a time-varying integer, and satisfies the following constraint

$$d_{\min} \leqslant d(k) \leqslant d_{\max} \tag{5}$$

where $d_{\min}$ and $d_{\max}$ are positive constants representing the minimum and maximum delays, respectively.

**Assumption 3.** The matrices $A$ and $B$ of system (4) have the following forms:

$$\boldsymbol{A} = \boldsymbol{A}_0 + \Delta\boldsymbol{A}, \quad \boldsymbol{B} = \boldsymbol{B}_0 + \Delta\boldsymbol{B} \tag{6}$$

where $A_0$ and $B_0$ are known constant matrices with appropriate dimensions, $\Delta A$ and $\Delta B$ real-valued unknown matrix functions representing norm-bounded parameter uncertainties satisfying

$$[\Delta\boldsymbol{A} \quad \Delta\boldsymbol{B}] = \boldsymbol{F}\varDelta(k)[\boldsymbol{J}_1 \quad \boldsymbol{J}_2] \tag{7}$$

where $\varDelta(k) \in \mathbf{R}^{\varDelta}$ is a real uncertain matrix function with Lévesque measureable elements satisfying $\varDelta^{\mathrm{T}}(k)\varDelta(k) \leqslant I$; $F$, $J_1$, and $J_2$ are known real constant matrices with appropriate dimensions.

## 3. Output tracking controller design

The purpose is to design a controller, so that the output $\boldsymbol{y}(k)$ tracks a reference signal $\boldsymbol{y}_{\mathrm{r}}(k)$ with the required $H_\infty$ output tracking performance. The reference signal $\boldsymbol{y}_{\mathrm{r}}(k) \in \mathbf{R}^q$ is generated by the following reference system:

$$\begin{cases} \boldsymbol{x}_{\mathrm{r}}(k+1) = \boldsymbol{A}_{\mathrm{r}}\boldsymbol{x}_{\mathrm{r}}(k) + \boldsymbol{B}_{\mathrm{r}}\boldsymbol{r}(k) \\ \boldsymbol{y}_{\mathrm{r}}(k) = \boldsymbol{C}_{\mathrm{r}}\boldsymbol{x}_{\mathrm{r}}(k) \end{cases} \tag{8}$$

where $\boldsymbol{x}_{\mathrm{r}}(k) \in \mathbf{R}^r$ is the reference state and $\boldsymbol{r}(k)$ the energy bounded reference input; $\boldsymbol{A}_{\mathrm{r}}$, $\boldsymbol{B}_{\mathrm{r}}$, and $\boldsymbol{C}_{\mathrm{r}}$ are known constant matrices with appropriate dimensions and $\boldsymbol{A}_{\mathrm{r}}$ is Hurwitz.

Consider the following state-feedback controller

$$\boldsymbol{u}(k) = \boldsymbol{K}_1\boldsymbol{x}(k - d(k)) + \boldsymbol{K}_2\boldsymbol{x}_{\mathrm{r}}(k) \tag{9}$$

where $\boldsymbol{K}_1$ and $\boldsymbol{K}_2$ are the control gains.

Define the tracking error as $\boldsymbol{e}(k) = \boldsymbol{y}(k) - \boldsymbol{y}_{\mathrm{r}}(k)$. To determine the $H_\infty$ output tracking performance of system (4), the augmented vector $\boldsymbol{z}(k) = \left[\boldsymbol{x}^{\mathrm{T}}(k) \quad \boldsymbol{x}_{\mathrm{r}}^{\mathrm{T}}(k)\right]^{\mathrm{T}}$ is defined. From Eqs. (4), (8) and (9), the following augmented system is obtained:

$$\begin{cases} \boldsymbol{z}(k+1) = \overline{\boldsymbol{A}}\boldsymbol{z}(k) + \overline{\boldsymbol{A}}_1\boldsymbol{z}(k-d(k)) + \overline{\boldsymbol{B}}\boldsymbol{v}(k) \\ \boldsymbol{e}(k) = \overline{\boldsymbol{C}}\boldsymbol{z}(k) + \overline{\boldsymbol{C}}_1\boldsymbol{z}(k-d(k)) \\ \boldsymbol{z}(k) = \boldsymbol{\phi}(k) \quad (k = -d_{\max}, -d_{\max}+1, \ldots, 0) \end{cases} \tag{10}$$

where $\boldsymbol{v}(k) = [\boldsymbol{w}^{\mathrm{T}}(k) \quad \boldsymbol{r}^{\mathrm{T}}(k)]^{\mathrm{T}}$, $\boldsymbol{\phi}(k)$ is an initial condition sequence, and

$$\begin{cases} \overline{\boldsymbol{A}} = \begin{bmatrix} \boldsymbol{A} & \boldsymbol{BK}_2 \\ \mathbf{0} & \boldsymbol{A}_{\mathrm{r}} \end{bmatrix}, \quad \overline{\boldsymbol{A}}_1 = \begin{bmatrix} \boldsymbol{BK}_1 & \mathbf{0} \\ \mathbf{0} & \mathbf{0} \end{bmatrix}, \quad \overline{\boldsymbol{B}} = \begin{bmatrix} \boldsymbol{E} & \mathbf{0} \\ \mathbf{0} & \boldsymbol{B}_{\mathrm{r}} \end{bmatrix} \\ \overline{\boldsymbol{C}} = [\boldsymbol{C} \quad \boldsymbol{DK}_2 - \boldsymbol{C}_{\mathrm{r}}], \quad \overline{\boldsymbol{C}}_1 = [\boldsymbol{DK}_1 \quad \mathbf{0}] \end{cases} \tag{11}$$

System (4) is said to have the $H_\infty$ output tracking performance for a scalar $\eta > 0$, if[14]

(a) The augmented system (10) with $\boldsymbol{v}(k) \equiv \mathbf{0}$ is asymptotically stable.

(b) Under zero initial condition, the following inequality holds for all nonzero $\boldsymbol{v}(k) \in L_2[0,\infty)$,

$$\|\boldsymbol{e}(k)\|_2 < \eta\|\boldsymbol{v}(k)\|_2 \tag{12}$$

The aforementioned requirements certificate that the effects of $\boldsymbol{w}(k)$ and $\boldsymbol{r}(k)$ on the tracking error $\boldsymbol{e}(k)$ are attenuated below a desired level in the $H_\infty$ sense.

From Conditions (a) and (b), it is known that the $H_\infty$ output tracking performance of system (4) is indicated by system (10). The following lemma plays a fundamental role in the output tracking controller design.

**Lemma 1.** *If there exist appropriately dimensioned matrices $P > \mathbf{0}, Q > \mathbf{0}, R > \mathbf{0}$, $Y$, $W$, $U$ satisfying the following inequality*

$$\tilde{\boldsymbol{\Omega}} < \mathbf{0} \tag{13}$$

*Then, system (10) with $v(k) \equiv \mathbf{0}$ is asymptotically stable and under zero initial condition $\|e(k)\|_2 < \eta\|v(k)\|_2$ holds for all nonzero $v(k) \in L_2[0,\infty)$.*

*$\boldsymbol{P} > \mathbf{0}$ means that $\boldsymbol{P}$ is real symmetric and positive definite, and $\tilde{\boldsymbol{\Omega}}$ in* Eq. (13) *has the following form:*

$$\tilde{\boldsymbol{\Omega}} = \begin{bmatrix} \boldsymbol{\Psi}_{11} & \boldsymbol{\Psi}_{12} & \overline{\boldsymbol{A}}^{\mathrm{T}}\boldsymbol{P}\overline{\boldsymbol{A}}/2 - \boldsymbol{Y} & \boldsymbol{\Psi}_{14} \\ * & \boldsymbol{\Psi}_{22} & \overline{\boldsymbol{A}}_1^{\mathrm{T}}\boldsymbol{P}\overline{\boldsymbol{A}}/2 - \boldsymbol{W} & \boldsymbol{\Psi}_{24} \\ * & * & -\boldsymbol{R}/d_{\max} & \overline{\boldsymbol{A}}^{\mathrm{T}}\boldsymbol{P}\overline{\boldsymbol{B}}/2 - \boldsymbol{U}^{\mathrm{T}} \\ * & * & * & \boldsymbol{\Psi}_{44} \end{bmatrix}$$

$$\boldsymbol{\Psi}_{11} = d_{\max}(\overline{\boldsymbol{A}} - \boldsymbol{I})^{\mathrm{T}}\boldsymbol{R}(\overline{\boldsymbol{A}} - \boldsymbol{I}) - \boldsymbol{P} + (d_{\max} - d_{\min} + 1)\boldsymbol{Q} + \boldsymbol{Y} + \boldsymbol{Y}^{\mathrm{T}} + \overline{\boldsymbol{C}}^{\mathrm{T}}\overline{\boldsymbol{C}}$$

$$\boldsymbol{\Psi}_{12} = \overline{\boldsymbol{A}}^{\mathrm{T}}\boldsymbol{P}(\overline{\boldsymbol{A}} + \overline{\boldsymbol{A}}_1)/2 + d_{\max}(\overline{\boldsymbol{A}} - \boldsymbol{I})^{\mathrm{T}}\boldsymbol{R}\overline{\boldsymbol{A}}_1 + \boldsymbol{W}^{\mathrm{T}} - \boldsymbol{Y} + \overline{\boldsymbol{C}}^{\mathrm{T}}\overline{\boldsymbol{C}}_1$$

$$\boldsymbol{\Psi}_{14} = \overline{\boldsymbol{A}}^{\mathrm{T}}\boldsymbol{P}\overline{\boldsymbol{B}}/2 + d_{\max}(\overline{\boldsymbol{A}} - \boldsymbol{I})^{\mathrm{T}}\boldsymbol{R}\overline{\boldsymbol{B}} + \boldsymbol{U}^{\mathrm{T}}$$

$$\boldsymbol{\Psi}_{22} = \overline{\boldsymbol{A}}_1^{\mathrm{T}}\boldsymbol{P}(\overline{\boldsymbol{A}} + \overline{\boldsymbol{A}}_1) + d_{\max}\overline{\boldsymbol{A}}_1^{\mathrm{T}}\boldsymbol{R}\overline{\boldsymbol{A}}_1 - \boldsymbol{Q} - \boldsymbol{W} - \boldsymbol{W}^{\mathrm{T}} + \overline{\boldsymbol{C}}_1^{\mathrm{T}}\overline{\boldsymbol{C}}_1$$

$$\boldsymbol{\Psi}_{24} = \overline{\boldsymbol{A}}^{\mathrm{T}}\boldsymbol{P}\overline{\boldsymbol{B}}/2 + \overline{\boldsymbol{A}}_1^{\mathrm{T}}\boldsymbol{P}\overline{\boldsymbol{B}} + d_{\max}\overline{\boldsymbol{A}}_1^{\mathrm{T}}\boldsymbol{R}\overline{\boldsymbol{B}} - \boldsymbol{U}^{\mathrm{T}}$$

$$\boldsymbol{\Psi}_{44} = \overline{\boldsymbol{B}}^{\mathrm{T}}\boldsymbol{P}\overline{\boldsymbol{B}} + d_{\max}\overline{\boldsymbol{B}}^{\mathrm{T}}\boldsymbol{R}\overline{\boldsymbol{B}} - \eta^2\boldsymbol{I}$$

**Proof.** The proof is divided into two parts:

(1) The asymptotic stability of system (10) with $v(k) \equiv \mathbf{0}$.

Let $y_{\mathrm{m}}(k) = z(k+1) - z(k)$. Choose the following Lyapunov-Krasovskii functional candidate:

$$V(k, z(k), d(k)) = V_1 + V_2 + V_3 + V_4 \tag{14}$$

where

$$V_1(k, \boldsymbol{z}(k)) = \boldsymbol{z}^{\mathrm{T}}(k)\boldsymbol{P}\boldsymbol{z}(k)$$

$$V_2(k, \boldsymbol{z}(k), d(k)) = \sum_{i=k-d(k)}^{k-1} \boldsymbol{z}^{\mathrm{T}}(i)\boldsymbol{Q}\boldsymbol{z}(i)$$

$$V_3(k, \boldsymbol{z}(k)) = \sum_{j=-d_{\max}+2}^{-d_{\min}-1} \sum_{i=k+j-1}^{k-1} \boldsymbol{z}^{\mathrm{T}}(i)\boldsymbol{Q}\boldsymbol{z}(i)$$

$$V_4(k, \boldsymbol{z}(k)) = \sum_{j=-d_{\max}}^{-1} \sum_{i=k+j}^{k-1} \boldsymbol{y}_{\mathrm{m}}^{\mathrm{T}}(i)\boldsymbol{R}\boldsymbol{y}_{\mathrm{m}}(i)$$

with $P$, $Q$, and $R$ being positive symmetrical matrices to be determined.

Since $z(k) - z(k-d(k)) - \sum_{i=k-d(k)}^{k-1} y_m(i) = \mathbf{0}$, Eq. (15) holds for any appropriately dimensioned matrices $Y$ and $W$.

$$2(\boldsymbol{z}^{\mathrm{T}}(k)\boldsymbol{Y} + \boldsymbol{z}^{\mathrm{T}}(k-d(k))\boldsymbol{W}) \cdot \left( \boldsymbol{z}(k) - \boldsymbol{z}(k-d(k)) - \sum_{i=k-d(k)}^{k-1} \boldsymbol{y}_{\mathrm{m}}(i) \right) = \mathbf{0} \tag{15}$$

Define $\Delta V = V(k+1) - V(k)$. From Eqs. (10) and (15), $\Delta V_1$ *is given by*

$$\begin{aligned}\Delta V_1 = \frac{1}{d(k)} \sum_{i=k-d(k)}^{k-1} \{ & \boldsymbol{z}^{\mathrm{T}}(k)(-\boldsymbol{P} + 2\boldsymbol{Y})\boldsymbol{z}(k) + \boldsymbol{z}^{\mathrm{T}}(k)[\overline{\boldsymbol{A}}^{\mathrm{T}}\boldsymbol{P}(\overline{\boldsymbol{A}} + \overline{\boldsymbol{A}}_1) \\ & + 2\boldsymbol{W}^{\mathrm{T}} - 2\boldsymbol{Y}]\boldsymbol{z}(k-d(k)) + \boldsymbol{z}^{\mathrm{T}}(k)(\overline{\boldsymbol{A}}^{\mathrm{T}}\boldsymbol{P}\overline{\boldsymbol{A}} - 2\boldsymbol{Y})d(k)\boldsymbol{y}_{\mathrm{m}}(i) \\ & + \boldsymbol{z}^{\mathrm{T}}(k-d(k))[\overline{\boldsymbol{A}}_1^{\mathrm{T}}\boldsymbol{P}(\overline{\boldsymbol{A}} + \overline{\boldsymbol{A}}_1) - 2\boldsymbol{W}]\boldsymbol{z}(k-d(k)) \\ & + \boldsymbol{z}^{\mathrm{T}}(k-d(k))(\overline{\boldsymbol{A}}_1^{\mathrm{T}}\boldsymbol{P}\overline{\boldsymbol{A}} - 2\boldsymbol{W})d(k)\boldsymbol{y}_{\mathrm{m}}(i)\}\end{aligned} \tag{16}$$

Furthermore,

$$\begin{aligned}\Delta V_2 &= \sum_{i=k-d(k+1)+1}^{k} \boldsymbol{z}^{\mathrm{T}}(i)\boldsymbol{Q}\boldsymbol{z}(i) - \sum_{i=k-d(k)}^{k-1} \boldsymbol{z}^{\mathrm{T}}(i)\boldsymbol{Q}\boldsymbol{z}(i) \\ &\leqslant \boldsymbol{z}^{\mathrm{T}}(k)\boldsymbol{Q}\boldsymbol{z}(k) - \boldsymbol{z}^{\mathrm{T}}(k-d(k))\boldsymbol{Q}\boldsymbol{z}(k-d(k)) \\ &\quad + \sum_{i=k-d_{\max}+1}^{k-d_{\min}} \boldsymbol{z}^{\mathrm{T}}(i)\boldsymbol{Q}\boldsymbol{z}(i)\end{aligned} \tag{17}$$

$$\begin{aligned}\Delta V_3 &= \sum_{j=-d_{\max}+2}^{-d_{\min}+1} \left( \sum_{i=k+j}^{k} \boldsymbol{z}^{\mathrm{T}}(i)\boldsymbol{Q}\boldsymbol{z}(i) - \sum_{i=k+j+1}^{k-1} \boldsymbol{z}^{\mathrm{T}}(i)\boldsymbol{Q}\boldsymbol{z}(i) \right) \\ &= (d_{\max} - d_{\min})\boldsymbol{z}^{\mathrm{T}}(k)\boldsymbol{Q}\boldsymbol{z}(k) - \sum_{i=k-d_{\max}+1}^{k-d_{\min}} \boldsymbol{z}^{\mathrm{T}}(i)\boldsymbol{Q}\boldsymbol{z}(i)\end{aligned} \tag{18}$$

$$\begin{aligned}\Delta V_4 &= \sum_{j=-d_{\max}}^{-1} (\boldsymbol{y}_{\mathrm{m}}^{\mathrm{T}}(k)\boldsymbol{R}\boldsymbol{y}_{\mathrm{m}}(k) - \boldsymbol{y}_{\mathrm{m}}^{\mathrm{T}}(k+j)\boldsymbol{R}\boldsymbol{y}_{\mathrm{m}}(k+j)) \\ &\leqslant d_{\max}\boldsymbol{z}^{\mathrm{T}}(k)(\overline{\boldsymbol{A}} - \boldsymbol{I})^{\mathrm{T}}\boldsymbol{R}(\overline{\boldsymbol{A}} - \boldsymbol{I})\boldsymbol{z}(k) \\ &\quad + 2d_{\max}\boldsymbol{z}^{\mathrm{T}}(k)(\overline{\boldsymbol{A}} - \boldsymbol{I})^{\mathrm{T}}\boldsymbol{R}\overline{\boldsymbol{A}}_1\boldsymbol{z}(k-d(k)) + d_{\max}\boldsymbol{z}^{\mathrm{T}}(k \\ &\quad - d(k))\overline{\boldsymbol{A}}_1^{\mathrm{T}}\boldsymbol{R}\overline{\boldsymbol{A}}_1\boldsymbol{z}(k-d(k)) - \sum_{i=k-d(k)}^{k-1} \boldsymbol{y}_{\mathrm{m}}^{\mathrm{T}}(i)\boldsymbol{R}\boldsymbol{y}_{\mathrm{m}}(i)\end{aligned} \tag{19}$$

Adding Eqs. (16)–(19) gives

$$\begin{aligned}\Delta V &= \Delta V_1 + \Delta V_2 + \Delta V_3 + \Delta V_4 \\ &\leqslant \frac{1}{d(k)} \sum_{i=k-d(k)}^{k-1} \bar{\xi}^{\mathrm{T}}(k,i)\overline{\boldsymbol{\Omega}}\bar{\xi}(k,i)\end{aligned} \tag{20}$$

where $\bar{\xi}^{\mathrm{T}}(k,i) = \begin{bmatrix} \boldsymbol{z}^{\mathrm{T}}(k) & \boldsymbol{z}^{\mathrm{T}}(k-d(k)) & d(k)\boldsymbol{y}_{\mathrm{m}}^{\mathrm{T}}(i) \end{bmatrix}$ and

$$\overline{\boldsymbol{\Omega}} = \begin{bmatrix} \boldsymbol{\Psi}_{11} & \boldsymbol{\Psi}_{12} & \overline{\boldsymbol{A}}^{\mathrm{T}}\boldsymbol{P}\overline{\boldsymbol{A}}/2 - \boldsymbol{Y} \\ * & \boldsymbol{\Psi}_{22} & \overline{\boldsymbol{A}}_1^{\mathrm{T}}\boldsymbol{P}\overline{\boldsymbol{A}}/2 - \boldsymbol{W} \\ * & * & -\boldsymbol{R}/d_{\max} \end{bmatrix} \tag{21}$$

From Eq. (20), we know that if

$$\overline{\boldsymbol{\Omega}} < \mathbf{0} \tag{22}$$

Then, $\Delta V < 0$ holds for all nonzero $\bar{\xi}(k,i)$, which means that system (10) is asymptotically stable with $v(t) \equiv \mathbf{0}$.

(2) Under zero initial condition, $\|e(k)\|_2 < \eta\|v(k)\|_2$ holds for all nonzero $v(k) \in L_2[0,\infty)$.

For any appropriately dimensioned matrix $Y$, $W$, and $U$, the following equation holds

$$2(\boldsymbol{z}^{\mathrm{T}}(k)\boldsymbol{Y} + \boldsymbol{z}^{\mathrm{T}}(k-d(k))\boldsymbol{W} + \boldsymbol{v}^{\mathrm{T}}(k)\boldsymbol{U}) \cdot \left( \boldsymbol{z}(k) - \boldsymbol{z}(k-d(k)) - \sum_{i=k-d(k)}^{k-1} \boldsymbol{y}_{\mathrm{m}}(i) \right) = 0 \tag{23}$$

By following the similar operations as earlier, we have

$$\Delta V \leqslant \frac{1}{d(k)} \sum_{i=k-d(k)}^{k-1} \xi^{\mathrm{T}}(k,i)\boldsymbol{\Omega}\xi(k,i) \tag{24}$$

where $\xi^{\mathrm{T}}(k,i) = \begin{bmatrix} \boldsymbol{z}^{\mathrm{T}}(k) & \boldsymbol{z}^{\mathrm{T}}(k-d(k)) & d(k)\boldsymbol{y}_{\mathrm{m}}^{\mathrm{T}}(i) & \boldsymbol{v}^{\mathrm{T}}(k) \end{bmatrix}$ and

$$\boldsymbol{\Omega} = \begin{bmatrix} \boldsymbol{\Omega}_{11} & \boldsymbol{\Omega}_{12} \\ * & \boldsymbol{\Omega}_{22} \end{bmatrix} \tag{25}$$

in which

$$\begin{cases} \boldsymbol{\Omega}_{11} = \begin{bmatrix} \boldsymbol{\Psi}_{11} & \boldsymbol{\Psi}_{12} \\ * & \boldsymbol{\Psi}_{22} \end{bmatrix}, \boldsymbol{\Omega}_{22} = \begin{bmatrix} -\boldsymbol{R}/d_{\max} & \overline{\boldsymbol{A}}^{\mathrm{T}}\boldsymbol{P}\overline{\boldsymbol{B}}/2 - \boldsymbol{U}^{\mathrm{T}} \\ * & \overline{\boldsymbol{B}}^{\mathrm{T}}\boldsymbol{P}\overline{\boldsymbol{B}} + d_{\max}\overline{\boldsymbol{B}}^{\mathrm{T}}\boldsymbol{R}\overline{\boldsymbol{B}} \end{bmatrix} \\ \boldsymbol{\Omega}_{12} = \begin{bmatrix} \overline{\boldsymbol{A}}^{\mathrm{T}}\boldsymbol{P}\overline{\boldsymbol{A}}/2 - \boldsymbol{Y} & \overline{\boldsymbol{A}}^{\mathrm{T}}\boldsymbol{P}\overline{\boldsymbol{B}}/2 + d_{\max}(\overline{\boldsymbol{A}} - \boldsymbol{I})^{\mathrm{T}}\boldsymbol{R}\overline{\boldsymbol{B}} + \boldsymbol{U}^{\mathrm{T}} \\ \overline{\boldsymbol{A}}_1^{\mathrm{T}}\boldsymbol{P}\overline{\boldsymbol{A}}/2 - \boldsymbol{W} & \overline{\boldsymbol{A}}^{\mathrm{T}}\boldsymbol{P}\overline{\boldsymbol{B}}/2 + (1 + d_{\max})\overline{\boldsymbol{A}}_1^{\mathrm{T}}\boldsymbol{R}\overline{\boldsymbol{B}} - \boldsymbol{U}^{\mathrm{T}} \end{bmatrix} \\ \boldsymbol{\Psi}_{11} = d_{\max}(\overline{\boldsymbol{A}} - \boldsymbol{I})^{\mathrm{T}}\boldsymbol{R}(\overline{\boldsymbol{A}} - \boldsymbol{I}) - \boldsymbol{P} + (d_{\max} - d_{\min} + 1)\boldsymbol{Q} + \boldsymbol{Y} + \boldsymbol{Y}^{\mathrm{T}} \\ \boldsymbol{\Psi}_{12} = \overline{\boldsymbol{A}}^{\mathrm{T}}\boldsymbol{P}(\overline{\boldsymbol{A}} + \overline{\boldsymbol{A}}_1)/2 + d_{\max}(\overline{\boldsymbol{A}} - \boldsymbol{I})^{\mathrm{T}}\boldsymbol{R}\overline{\boldsymbol{A}}_1 + \boldsymbol{W}^{\mathrm{T}} - \boldsymbol{Y} \\ \boldsymbol{\Psi}_{22} = \overline{\boldsymbol{A}}_1^{\mathrm{T}}\boldsymbol{P}(\overline{\boldsymbol{A}} + \overline{\boldsymbol{A}}_1) + d_{\max}\overline{\boldsymbol{A}}_1^{\mathrm{T}}\boldsymbol{R}\overline{\boldsymbol{A}}_1 - \boldsymbol{Q} - \boldsymbol{W} - \boldsymbol{W}^{\mathrm{T}} \end{cases} \tag{26}$$

Consider the following index:

$$\kappa = \sum_{\rho=0}^{\infty} (\boldsymbol{e}^{\mathrm{T}}(\rho)\boldsymbol{e}(\rho) - \eta^2\boldsymbol{v}^{\mathrm{T}}(\rho)\boldsymbol{v}(\rho)) \tag{27}$$

Under zero-initial conditions, $V(0,z(0),d(0)) = 0$ and $V(\infty, z(\infty), d(\infty)) > 0$, which leads to

$$\begin{aligned}\kappa &= \sum_{\rho=0}^{\infty} (\boldsymbol{e}^{\mathrm{T}}(\rho)\boldsymbol{e}(\rho) - \eta^2\boldsymbol{v}^{\mathrm{T}}(\rho)\boldsymbol{v}(\rho) + \Delta V) - V(\infty) \\ &\leqslant \sum_{\rho=0}^{\infty} (\boldsymbol{e}^{\mathrm{T}}(\rho)\boldsymbol{e}(\rho) - \eta^2\boldsymbol{v}^{\mathrm{T}}(\rho)\boldsymbol{v}(\rho) + \Delta V)\end{aligned} \tag{28}$$

Substituting Eq. (24) into Eq. (28), while considering the second equation in Eq. (10), gives

$$\begin{aligned}&\boldsymbol{e}^{\mathrm{T}}(\rho)\boldsymbol{e}(\rho) - \eta^2\boldsymbol{v}^{\mathrm{T}}(\rho)\boldsymbol{v}(\rho) + \Delta V \\ &\leqslant \frac{1}{d(k)} \sum_{i=k-d(k)}^{k-1} \xi^{\mathrm{T}}(k,i)\widetilde{\boldsymbol{\Omega}}\xi(k,i)\end{aligned} \tag{29}$$

where $\widetilde{\boldsymbol{\Omega}}$ is defined in Eq. (13).

From Eq. (13), we have for all nonzero $v(k) \in L_2[0,\infty)$,

$$\boldsymbol{e}^{\mathrm{T}}(\rho)\boldsymbol{e}(\rho) - \eta^2\boldsymbol{v}^{\mathrm{T}}(\rho)\boldsymbol{v}(\rho) + \Delta V < 0 \tag{30}$$

which means $\kappa < 0$. Therefore, It can be concluded that for all non-zero $v(k) \in L_2[0,\infty)$, $\|e(k)\|_2 < \eta\|v(k)\|_2$ holds. The proof is completed. □

Based on Lemma 1, the $H_\infty$ output tracking controller is designed for the nominal system via Lemma 2.

**Lemma 2.** *There exists a state-feedback controller in the form of Eq. (9) so that system (4) achieves the* $H_\infty$ *output tracking* *performance $\eta$, if there exist appropriately dimensioned matrices $P>\mathbf{0}$, $Q>\mathbf{0}$, $R>\mathbf{0}$, $L>\mathbf{0}$, $S>0$, $Y$, $W$, and $U$, satisfying Eqs. (31) and (32).*

$$\begin{bmatrix} \boldsymbol{\Theta}_{11} & \boldsymbol{\Theta}_{12} \\ \boldsymbol{\Theta}_{12}^{\mathrm{T}} & \boldsymbol{\Theta}_{22} \end{bmatrix} < \mathbf{0} \tag{31}$$

$$\boldsymbol{RL}=\boldsymbol{I},\ \boldsymbol{PS}=\boldsymbol{I} \tag{32}$$

*where*

$$\begin{cases} \boldsymbol{\Theta}_{11}=\begin{bmatrix} \boldsymbol{\theta}_{11} & \boldsymbol{W}^{\mathrm{T}}-\boldsymbol{Y} & -\boldsymbol{Y} & \boldsymbol{U}^{\mathrm{T}} \\ * & \boldsymbol{\theta}_{22} & -\boldsymbol{W} & -\boldsymbol{U}^{\mathrm{T}} \\ * & * & -\boldsymbol{R}/d_{\max} & -\boldsymbol{U}^{\mathrm{T}} \\ * & * & * & -\eta^2\boldsymbol{I} \end{bmatrix} \\ \boldsymbol{\Theta}_{12}=\begin{bmatrix} \overline{\boldsymbol{A}}^{\mathrm{T}}-\boldsymbol{I} & \overline{\boldsymbol{A}}^{\mathrm{T}} & \mathbf{0} & \overline{\boldsymbol{C}}^{\mathrm{T}} \\ \overline{\boldsymbol{A}}_1^{\mathrm{T}} & \overline{\boldsymbol{A}}^{\mathrm{T}}+\overline{\boldsymbol{A}}_1^{\mathrm{T}} & \overline{\boldsymbol{A}}_1^{\mathrm{T}} & \overline{\boldsymbol{C}}_1^{\mathrm{T}} \\ \mathbf{0} & \overline{\boldsymbol{A}}^{\mathrm{T}} & \mathbf{0} & \mathbf{0} \\ \overline{\boldsymbol{B}}^{\mathrm{T}} & \overline{\boldsymbol{B}}^{\mathrm{T}} & \overline{\boldsymbol{B}}^{\mathrm{T}} & \mathbf{0} \end{bmatrix} \\ \boldsymbol{\Theta}_{22}=\begin{bmatrix} -\boldsymbol{L}/d_{\max} & \mathbf{0} & \mathbf{0} & \mathbf{0} \\ * & -\boldsymbol{S} & \mathbf{0} & \mathbf{0} \\ * & * & -\boldsymbol{S} & \mathbf{0} \\ * & * & * & -\boldsymbol{I} \end{bmatrix} \\ \boldsymbol{\theta}_{11}=(d_{\max}-d_{\min}+1)\boldsymbol{Q}-\boldsymbol{P}-\boldsymbol{P}^{\mathrm{T}}+\boldsymbol{Y}+\boldsymbol{Y}^{\mathrm{T}} \\ \boldsymbol{\theta}_{22}=-\boldsymbol{Q}-\boldsymbol{W}-\boldsymbol{W}^{\mathrm{T}} \end{cases} \tag{33}$$

**Proof.** Replace $P$ in Eq. (13) by $2P$. Substitute the following equation into Eq. (13):

$$\begin{aligned} &\overline{\boldsymbol{A}}_1^{\mathrm{T}}\boldsymbol{P}(\overline{\boldsymbol{A}}+\overline{\boldsymbol{A}}_1)+(\overline{\boldsymbol{A}}+\overline{\boldsymbol{A}}_1)^{\mathrm{T}}\boldsymbol{P}\overline{\boldsymbol{A}}_1 \\ &\quad=(\overline{\boldsymbol{A}}+\overline{\boldsymbol{A}}_1)^{\mathrm{T}}\boldsymbol{P}(\overline{\boldsymbol{A}}+\overline{\boldsymbol{A}}_1)+\overline{\boldsymbol{A}}_1^{\mathrm{T}}\boldsymbol{P}\overline{\boldsymbol{A}}_1-\overline{\boldsymbol{A}}^{\mathrm{T}}\boldsymbol{P}\overline{\boldsymbol{A}} \end{aligned} \tag{34}$$

By several Schur complement operations, Eq. (13) is equivalent to

$$\begin{bmatrix} \boldsymbol{\Theta}_{11}-\boldsymbol{\Gamma}^{\mathrm{T}}\boldsymbol{\Lambda}\boldsymbol{\Gamma} & \overline{\boldsymbol{\Theta}}_{12} \\ \overline{\boldsymbol{\Theta}}_{12}^{\mathrm{T}} & \overline{\boldsymbol{\Theta}}_{22} \end{bmatrix} < \mathbf{0} \tag{35}$$

where

$$\boldsymbol{\Gamma}=\begin{bmatrix} \overline{\boldsymbol{A}} & \mathbf{0} & \mathbf{0} & \mathbf{0} \\ \mathbf{0} & \overline{\boldsymbol{A}} & \overline{\boldsymbol{A}} & \mathbf{0} \\ \mathbf{0} & \mathbf{0} & \overline{\boldsymbol{A}} & \mathbf{0} \\ \mathbf{0} & \mathbf{0} & \mathbf{0} & \mathbf{0} \end{bmatrix},\quad \boldsymbol{\Lambda}=\begin{bmatrix} \boldsymbol{P} & \mathbf{0} & \mathbf{0} & \mathbf{0} \\ * & \boldsymbol{P} & \mathbf{0} & \mathbf{0} \\ * & * & \boldsymbol{P} & \mathbf{0} \\ * & * & * & \boldsymbol{I} \end{bmatrix}$$

$$\overline{\boldsymbol{\Theta}}_{12}=\begin{bmatrix} (\overline{\boldsymbol{A}}^{\mathrm{T}}-\boldsymbol{I})\boldsymbol{R} & \overline{\boldsymbol{A}}^{\mathrm{T}}\boldsymbol{P} & \mathbf{0} & \overline{\boldsymbol{C}}^{\mathrm{T}} \\ \overline{\boldsymbol{A}}_1^{\mathrm{T}}\boldsymbol{R} & (\overline{\boldsymbol{A}}^{\mathrm{T}}+\overline{\boldsymbol{A}}_1^{\mathrm{T}})\boldsymbol{P} & \overline{\boldsymbol{A}}_1^{\mathrm{T}}\boldsymbol{P} & \overline{\boldsymbol{C}}_1^{\mathrm{T}} \\ \mathbf{0} & \overline{\boldsymbol{A}}^{\mathrm{T}}\boldsymbol{P} & \mathbf{0} & \mathbf{0} \\ \overline{\boldsymbol{B}}^{\mathrm{T}}\boldsymbol{R} & \overline{\boldsymbol{B}}^{\mathrm{T}}\boldsymbol{P} & \overline{\boldsymbol{B}}^{\mathrm{T}}\boldsymbol{P} & \mathbf{0} \end{bmatrix}$$

$$\overline{\boldsymbol{\Theta}}_{22}=\begin{bmatrix} -\boldsymbol{R}/d_{\max} & \mathbf{0} & \mathbf{0} & \mathbf{0} \\ * & -\boldsymbol{P} & \mathbf{0} & \mathbf{0} \\ * & * & -\boldsymbol{P} & \mathbf{0} \\ * & * & * & -\boldsymbol{I} \end{bmatrix}$$

As $\Lambda$ is positive definite, Eq. (35) holds, providing that the following equation holds:

$$\begin{bmatrix} \boldsymbol{\Theta}_{11} & \overline{\boldsymbol{\Theta}}_{12} \\ \overline{\boldsymbol{\Theta}}_{12}^{\mathrm{T}} & \boldsymbol{\Theta}_{22}^{-1} \end{bmatrix} < \mathbf{0} \tag{36}$$

Performing a congruence transformation to Eq. (36) by diag $(I_{n+r}, I_{n+r}, I_{n+r}, I_{l+r}, R^{-1}, P^{-1}, P^{-1}, I_q)$ together with the condition defined in Eq. (32), we obtain Eq. (31). The proof is completed. □

For uncertain system (4) satisfying Assumptions 2 and 3, the robust $H_\infty$ output tracking controller design is presented in Theorem 1. Lemmas 3 and 4 are recalled to establish the theorem.

**Lemma 3** [15]. *Given appropriately dimensioned matrices $\boldsymbol{H}$, $\boldsymbol{J}$, and $\boldsymbol{F}$, with $\boldsymbol{H}^T=\boldsymbol{H}$, then*

$$\boldsymbol{H}+\boldsymbol{F}\boldsymbol{\Delta}(k)\boldsymbol{J}+\boldsymbol{J}^{\mathrm{T}}\boldsymbol{\Delta}^{\mathrm{T}}(k)\boldsymbol{F}^{\mathrm{T}}<\mathbf{0} \tag{37}$$

*holds for all $\Delta(k)$ satisfying $\Delta^{\mathrm{T}}(k)\Delta(k)\leqslant I$ if and only if for some $\lambda>0$, Eq. (38) holds.*

$$\boldsymbol{H}+\lambda\boldsymbol{F}\boldsymbol{F}^{\mathrm{T}}+\lambda^{-1}\boldsymbol{J}^{\mathrm{T}}\boldsymbol{J}<\mathbf{0} \tag{38}$$

**Lemma 4** [15]. *If the LMI*

$$\begin{bmatrix} \boldsymbol{P} & \boldsymbol{I} \\ \boldsymbol{I} & \boldsymbol{L} \end{bmatrix} \geqslant \mathbf{0} \tag{39}$$

*is feasible in the $n\times n$ matrix variables $P>\mathbf{0}$ and $L>\mathbf{0}$, then* $\mathrm{tr}(PL)\geqslant n$; $\mathrm{tr}(PL)=n$ *if and only if $PL=I$.*

**Theorem 1.** *There exists a state-feedback controller in the form of* Eq. (9) *so that system* (4) *with uncertainties achieves the $H_\infty$ output tracking performance $\eta$, if there exist appropriately dimensioned matrices $P>\mathbf{0}$, $Q>\mathbf{0}$, $R>\mathbf{0}$, $L>\mathbf{0}$, $S>\mathbf{0}$, $Y$, $W$, $U$, and a scalar $\lambda>0$ satisfying the following equations:*

$$\begin{bmatrix} \boldsymbol{\Theta}_{11} & \widetilde{\boldsymbol{\Theta}}_{12} & \widetilde{\boldsymbol{J}}^{\mathrm{T}} \\ * & \widetilde{\boldsymbol{\Theta}}_{22} & \mathbf{0} \\ * & * & \widetilde{\boldsymbol{\Theta}}_{33} \end{bmatrix} < \mathbf{0} \tag{40}$$

$$\begin{bmatrix} \boldsymbol{R} & \boldsymbol{I} \\ \boldsymbol{I} & \boldsymbol{L} \end{bmatrix} \geqslant \mathbf{0},\quad \begin{bmatrix} \boldsymbol{P} & \boldsymbol{I} \\ \boldsymbol{I} & \boldsymbol{S} \end{bmatrix} \geqslant \mathbf{0} \tag{41}$$

$$\mathrm{tr}(\boldsymbol{RL}+\boldsymbol{PS})=2(n+r) \tag{42}$$

*where*

$$\begin{cases} \widetilde{\boldsymbol{\Theta}}_{12}=\begin{bmatrix} \overline{\boldsymbol{A}}_0^{\mathrm{T}}-\boldsymbol{I} & \overline{\boldsymbol{A}}_0^{\mathrm{T}} & \mathbf{0} & \overline{\boldsymbol{C}}^{\mathrm{T}} \\ \overline{\boldsymbol{A}}_{10}^{\mathrm{T}} & \overline{\boldsymbol{A}}_0^{\mathrm{T}}+\overline{\boldsymbol{A}}_{10}^{\mathrm{T}} & \overline{\boldsymbol{A}}_{10}^{\mathrm{T}} & \overline{\boldsymbol{C}}_1^{\mathrm{T}} \\ \mathbf{0} & \overline{\boldsymbol{A}}_0^{\mathrm{T}} & \mathbf{0} & \mathbf{0} \\ \overline{\boldsymbol{B}}^{\mathrm{T}} & \overline{\boldsymbol{B}}^{\mathrm{T}} & \overline{\boldsymbol{B}}^{\mathrm{T}} & \mathbf{0} \end{bmatrix} \\ \widetilde{\boldsymbol{\Theta}}_{22}=\begin{bmatrix} -\boldsymbol{L}/d_{\max}+\lambda\overline{\boldsymbol{F}}\overline{\boldsymbol{F}}^{\mathrm{T}} & \lambda\overline{\boldsymbol{F}}\overline{\boldsymbol{F}}^{\mathrm{T}} & \mathbf{0} & \mathbf{0} \\ * & -\boldsymbol{S}+2\lambda\overline{\boldsymbol{F}}\overline{\boldsymbol{F}}^{\mathrm{T}} & \mathbf{0} & \mathbf{0} \\ * & * & -\boldsymbol{S}+\lambda\overline{\boldsymbol{F}}\overline{\boldsymbol{F}}^{\mathrm{T}} & \mathbf{0} \\ * & * & * & -\boldsymbol{I} \end{bmatrix} \\ \widetilde{\boldsymbol{\Theta}}_{33}=\begin{bmatrix} -\lambda\boldsymbol{I} & \mathbf{0} & \mathbf{0} \\ * & -\lambda\boldsymbol{I} & \mathbf{0} \\ * & * & -\lambda\boldsymbol{I} \end{bmatrix},\ \overline{\boldsymbol{A}}_0=\begin{bmatrix} \boldsymbol{A}_0 & \boldsymbol{B}_0\boldsymbol{K}_2 \\ \mathbf{0} & \boldsymbol{A}_{\mathrm{r}} \end{bmatrix},\ \overline{\boldsymbol{A}}_{10}=\begin{bmatrix} \boldsymbol{B}_0\boldsymbol{K}_1 & \mathbf{0} \\ \mathbf{0} & \mathbf{0} \end{bmatrix} \\ \overline{\boldsymbol{F}}^{\mathrm{T}}=\begin{bmatrix} \boldsymbol{F}^{\mathrm{T}} & \mathbf{0} \end{bmatrix} \\ \widetilde{\boldsymbol{J}}=\begin{bmatrix} \overline{\boldsymbol{J}}_1 & \overline{\boldsymbol{J}}_2 & \mathbf{0} & \mathbf{0} \\ \mathbf{0} & \overline{\boldsymbol{J}}_1 & \overline{\boldsymbol{J}}_1 & \mathbf{0} \\ \mathbf{0} & \overline{\boldsymbol{J}}_2 & \mathbf{0} & \mathbf{0} \end{bmatrix},\ \overline{\boldsymbol{J}}_1=[\boldsymbol{J}_1\ \ \boldsymbol{J}_2\boldsymbol{K}_2],\ \overline{\boldsymbol{J}}_2=[\boldsymbol{J}_2\boldsymbol{K}_1\ \ \mathbf{0}] \end{cases} \tag{43}$$

**Proof.** Substituting Eqs. (6) and (7) into Eq. (11) yields

$$\overline{A} = \overline{A}_0 + \overline{F}\Delta(k)\overline{J}_1, \quad \overline{A}_1 = \overline{A}_{10} + \overline{F}\Delta(k)\overline{J}_2 \tag{44}$$

Substituting Eq. (44) into Eq. (31) gives

$$\widetilde{H} + \begin{bmatrix} \mathbf{0} \\ \widetilde{F} \end{bmatrix} \widetilde{\Delta}(k) [\widetilde{J} \quad \mathbf{0}] + [\widetilde{J} \quad \mathbf{0}]^{\mathrm{T}} \widetilde{\Delta}^{\mathrm{T}}(k) \begin{bmatrix} \mathbf{0} \\ \widetilde{F} \end{bmatrix}^{\mathrm{T}} < \mathbf{0} \tag{45}$$

where

$$\widetilde{H} = \begin{bmatrix} \boldsymbol{\Theta}_{11} & \widetilde{\boldsymbol{\Theta}}_{12} \\ \widetilde{\boldsymbol{\Theta}}_{12}^{\mathrm{T}} & \boldsymbol{\Theta}_{22} \end{bmatrix} < \mathbf{0}, \quad \widetilde{\Delta}(k) = \mathrm{diag}(\Delta(k), \Delta(k), \Delta(k)),$$

$$\widetilde{F}^{\mathrm{T}} = \begin{bmatrix} \overline{F}^{\mathrm{T}} & \overline{F}^{\mathrm{T}} & \mathbf{0} & \mathbf{0} \\ \mathbf{0} & \overline{F}^{\mathrm{T}} & \mathbf{0} & \mathbf{0} \\ \mathbf{0} & \mathbf{0} & \overline{F}^{\mathrm{T}} & \mathbf{0} \end{bmatrix}$$

Based on Lemma 3 and a Schur complement operation, Eq. (45) holds if and only if for some $\lambda > 0$ Eq. (40) holds. Then, with the conditions that $RL = I, PS = I$, Eq. (40) is equivalent to Eq. (31).

By Lemma 4, Eq. (32) is equivalent to Eqs. (41) and (42). The proof is completed. □

## 4. Simulation results

In this section, two examples are provided to demonstrate the effectiveness of the proposed delay-dependent criterion and the corresponding controller design approach.

### 4.1. Numerical example

Consider the following discrete-time model of an inverted pendulum system:

$$\boldsymbol{x}(k+1) = \begin{bmatrix} 1.0078 & 0.0301 \\ 0.5202 & 1.0078 \end{bmatrix} \boldsymbol{x}(k) + \begin{bmatrix} -0.0001 \\ -0.0053 \end{bmatrix} \boldsymbol{u}(k) \tag{46}$$

The sampling time is $T_s = 30$ ms. The system is used to compare the results with those in Ref. [16]. The delayed controller (47) is used to stabilize system (46).

$$\boldsymbol{u}(k) = [110.6827 \quad 34.6980]\boldsymbol{x}(k - d(k)) \tag{47}$$

The lower delay bound is set as $d_{\min} = 1$. According to the result of Ref. [16], the maximum allowable upper bound $d_{\max}^* = 5$. By using Lemma 2, it is calculated that $d_{\max}^* = 6$. To demonstrate the result clearly, in the simulation, the time delay $d(k)$ is set to be a constant integer. Figs. 2–4 illustrate the stability degradation of the closed-loop system in which $x_1$ and $x_2$ denote the components of $\boldsymbol{x}(k)$.

Our results are slightly less conservative. Note that in some cases it makes sense to find a balance between $d_{\max}^*$ and the tracking performance. According to Theorem 1, the proposed approach can provide a suitable $d_{\max}^*$ and at the same time satisfy the $H_\infty$ output tracking performance.

**Remark 1.** For a given lower delay bound $d_{\min}$, there exists a maximum upper delay bound $d_{\max}^*$. $d_{\max}^*$ is used to evaluate the conservatism of delay-dependent stability criteria.[16]

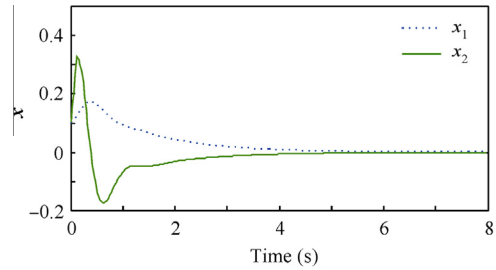


**Fig. 2** Closed-loop response with $d = 4$.

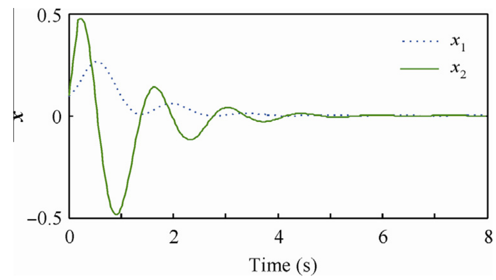


**Fig. 3** Closed-loop response with $d = 6$.

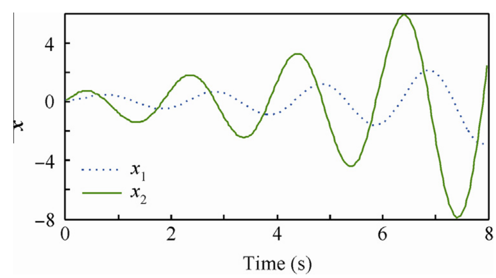


**Fig. 4** Closed-loop response with $d = 8$.

### 4.2. Application to HIRM aircraft

#### 4.2.1. HIRM system description

The output tracking controller is applied to the HIRM. The HIRM was originally developed under a Defense Evaluation and Research Agency program as a vehicle for high angle-of-attack aerodynamic investigations. The origin of the model explains the unconventional configuration with both canard and tailplane plus an elongated nose.[17] The configuration of the HIRM is shown in Ref. [18].

The rigid body equations of motion and transformations between the various axial systems used in the mathematical model are standard.[17]

A linearization of the longitudinal dynamics of the HIRM about Mach number 0.3 and an altitude of 1600 m is used. The continuous-time system is shown as follows:

$$\dot{\boldsymbol{x}}(t) = \begin{bmatrix} -0.5427 & 1 & 0 \\ -1.069 & -0.4134 & 0 \\ 0 & 1 & 0 \end{bmatrix} \boldsymbol{x}(t) + \begin{bmatrix} -0.113 \\ -3.259 \\ 0 \end{bmatrix} \boldsymbol{u}(t) + \begin{bmatrix} 1 \\ 0 \\ 0 \end{bmatrix} \boldsymbol{w}(t) \tag{48}$$

Muir [17] put forward the benchmark problems for the HIRM control system. For linear assessments, the control laws need to be robust to $\pm 10\%$ modeling errors in the aerodynamics derivatives. By adding the uncertainties into the individual state-space matrix elements,[19] the continuous-time perturbation system is obtained.

The normal system (48) and the perturbation system are discretized on a sampling time of 25 ms.[20] The discrete-time system matrices in Eqs. (6) and (7) are shown as follows:

$$\begin{cases} \boldsymbol{A}_0 = \begin{bmatrix} 0.9862 & 0.0243 & 0 \\ -0.0264 & 0.9894 & 0 \\ -0.0030 & 0.0249 & 1.0000 \end{bmatrix}, \quad \boldsymbol{B}_0 = \begin{bmatrix} -0.0038 \\ -0.0810 \\ -0.0010 \end{bmatrix}, \\ \boldsymbol{E} = [0.0230 \quad 0 \quad 0]^{\mathrm{T}} \\ \Delta\boldsymbol{A} = \pm \begin{bmatrix} 0.0014 & 0.0004 & 0 \\ 0.0026 & 0.0011 & 0 \\ 0 & 0 & 0 \end{bmatrix}, \quad \Delta\boldsymbol{B} = \pm \begin{bmatrix} 0.0004 \\ 0.0080 \\ 0 \end{bmatrix} \end{cases} \tag{49}$$

For the sake of controller design, the pair $(\Delta\boldsymbol{A}, \Delta\boldsymbol{B})$ should be decomposed in the form of Eq. (7). To show the robustness of the controller, the uncertainties used in the following design and simulation are slightly enhanced. The uncertainties are set as follows:

$$\boldsymbol{F} = [0.04 \quad 0.8 \quad 0]^{\mathrm{T}}, \quad \boldsymbol{J}_1 = [0.033 \quad 0.014 \quad 0], \quad \boldsymbol{J}_2 = 0.1 \tag{50}$$

$$\varDelta(k) = \begin{cases} 0.15, & 0 \leqslant k < 20 \\ -0.15, & 20 \leqslant k \leqslant 40 \end{cases} \tag{51}$$

Suppose that the system is influenced by a disturbance of harmonics wind gust. In the simulation, the disturbance $\boldsymbol{w}(k)$ is generated by an exogenous system described by

$$\begin{cases} \boldsymbol{\mu}(k+1) = \begin{bmatrix} 0.9922 & 0.1247 \\ -0.1247 & 0.9922 \end{bmatrix} \boldsymbol{\mu}(k) \\ \boldsymbol{w}(k) = [25 \quad 0]\,\boldsymbol{\mu}(k) \end{cases} \tag{52}$$

The initial value of the disturbance is 0.1. It is reported in Ref. [21] that many kinds of disturbances in engineering can be described by this model, for example, unknown constant and harmonics with unknown phase and magnitude.

*4.2.2. Controller design and evaluation*

Suppose the reference model is given by

$$\boldsymbol{A}_{\mathrm{m}} = \begin{bmatrix} 0.9878 & 0.0189 & -0.0056 \\ 0.0085 & 0.8736 & -0.0056 \\ 0.0001 & 0.0235 & 0.9985 \end{bmatrix}, \quad \boldsymbol{B}_{\mathrm{m}} = \begin{bmatrix} 0.0056 \\ 0.1190 \\ 0.0015 \end{bmatrix}, \quad \boldsymbol{C}_{\mathrm{m}} = \boldsymbol{C} \tag{53}$$

By applying Theorem 1 in this paper and Algorithm 1,[12] the delayed controller is as follows:

$$\begin{aligned} \boldsymbol{u}(k) = {} & [-0.5054 \quad 3.3877 \quad 3.1151]\,\boldsymbol{x}(k - d(k)) \\ & + [0.2474 \quad -3.2382 \quad -3.1120]\,\boldsymbol{x}_{\mathrm{r}}(k) \end{aligned} \tag{54}$$

In the simulation, the time delay $d(k)$ is generated randomly, which is shown in Fig. 5.

The controller is compared with a dynamic output feedback sliding-mode (DFSM) controller.[21] The state responses of the nominal closed-loop system are shown in Fig. 6. The results for the uncertainties and the disturbance are shown in Fig. 7.

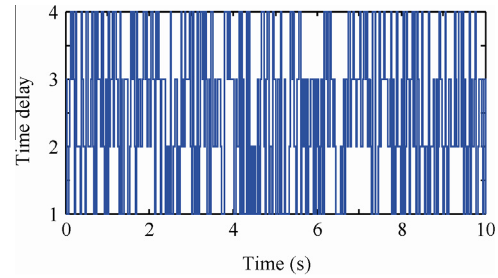


**Fig. 5** Time delay.

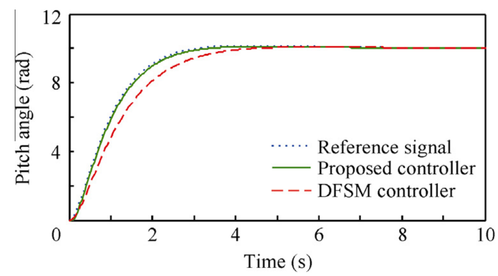


**Fig. 6** Closed-loop response (nominal case).

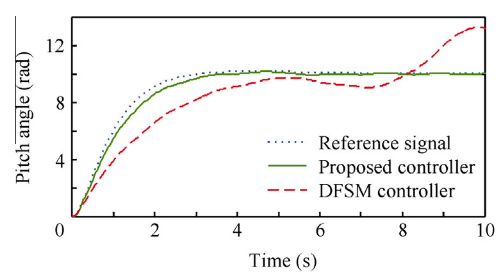


**Fig. 7** Closed-loop response (uncertain case).

From Fig. 6, it can be seen that both of the two controllers achieve good performance in despite of the time delay, and the output tracking of the proposed controller is closer to the reference output compared with the DFSM controller.

Fig. 7 demonstrates the performances of the two controllers with considerations of the uncertainties and the disturbance. The proposed controller remains good tracking performance which illustrates the effectiveness of the proposed approach.

## 5. Conclusions

(1) The $H_\infty$ output tracking for flight control systems with interval time-varying delay is investigated. The delay-dependent sufficient criterion is related not only to the delay interval but also to the minimum delay, which indicates that more specific information is led into the controller design procedure. The criterion is represented by LMIs.

(2) The simulation for the HIRM is given to show the effectiveness of the proposed tracking controller design approach. Compared with a delay-free controller, the proposed controller has better tracking performances.

**Acknowledgements**

The authors are grateful to the anonymous reviewers for their critical and constructive reviews of the manuscript. This study was supported by the National Natural Science Foundation of China (Nos: 61074027 and 61273083).

**References**

1. Wang LD, Zhai CR, Jin WR, Zhan XQ. Enhanced GPS measurements simulation for space-oriented navigation system design. *Chin J Aeronaut* 2010;**23**(4):438–46.
2. Xu L, Wang Q, Li W, Hou Y. Stability analysis and stabilisation of full-envelope networked flight control systems: switched system approach. *IET Control Theory Appl* 2012;**6**(2):286–96.
3. Ionita A. Input delay investigation in the short period flying qualities criteria; 1996. Report No.: AIAA-1996-3424.
4. Tan WQ, Efremov AV, Qu XJ. A criterion based on closed-loop pilot–aircraft systems for predicting flying qualities. *Chin J Aeronaut* 2010;**23**(5):511–7.
5. Gao SL, Li R, Huang ZG. A fault-tolerance estimating method for ionosphere corrections in satellite navigation system. *Chin J Aeronaut* 2011;**24**(6):749–55.
6. Sun J, Liu GP, Chen J, Rees D. Improved delay-range-dependent stability criteria for linear systems with time-varying delays. *Automatica* 2010;**46**(2):466–70.
7. Zecevic AI, Siljak DD. Estimating the region of attraction for large-scale systems with uncertainties. *Automatica* 2010;**46**(2):445–51.
8. Li HP, Shi Y. Robust $H_\infty$ filtering for nonlinear stochastic systems with uncertainties and Markov delays. *Automatica* 2012;**48**(1):159–66.
9. Pai MC. Design of adaptive sliding mode controller for robust tracking and model following. *J Franklin Inst* 2010;**347**(10):1837–49.
10. Atesoglu O, Ozgoren MK. Control and robustness analysis for a High-$\alpha$ maneuverable thrust-vectoring fighter aircraft. *J Guid Control Dyn* 2009;**32**(5):1483–96.
11. Bresch-Pietri D, Krstic M. Adaptive trajectory tracking despite unknown input delay and plant parameters. *Automatica* 2009;**45**(9):2074–81.
12. Wang Q, Zhang YZ, Dong CY, Ni ML. Robust trajectory tracking of unstable aircraft with measurement delay. *Proc IMechE, Part I: J Syst Control Eng* 2012;**226**(9):1220–30.
13. Wu ST, Fei YH. *Flight control system*. Beijing: Beihang University Press; 2006 [Chinese].
14. Gao HJ, Chen TW. Network-based $H_\infty$ output tracking control. *IEEE Trans Autom Control* 2008;**53**(3):655–67.
15. Xu SY, van Dooren P, Stefan R, Lam L. Robust stability and stabilization for singular systems with state delay and parameter uncertainty. *IEEE Trans Autom Control* 2002;**47**(7):1122–8.
16. Zhang BY, Xu SY, Zou Y. Improved stability criterion and its applications in delayed controller design for discrete-time systems. *Automatica* 2008;**44**(11):2963–7.
17. Muir E. The Garteur high incidence research model (HIRM) benchmark problem; 1998. Report No.: AIAA-1998-4243.
18. Ross AJ, Edwards GF, Klein V, Batterson JG. Validation of aerodynamic parameters for high-incidence research models. *J Aircr* 1989;**26**(7):621–8.
19. Markerink J. HIRM design of a robust, scheduled controller using $\mu$-synthesis; 1998. Report No.: AIAA-1998-4246.
20. Lai NO, Edwards C, Spurgeon SK. On output tracking using dynamic output feedback discrete-time sliding-mode controllers. *IEEE Trans Autom Control* 2007;**52**(10):1975–81.
21. Guo L, Chen WH. Disturbance attenuation and rejection for systems with nonlinearity via DOBC approach. *Int J Robust Nonlinear Control* 2005;**15**(3):109–25.

**Zhang Yingxin** works at the Second System Design Department of the Second Research Academy of CASIC. She received her Doctor's degree in School of Automation Science and Electrical Engineering at Beihang University in 2013. Her area of research includes guidance and control of aircraft, time-delay systems, and robust control.

**Wang Qing** is a professor and Ph.D. advisor in the School of Automation Science and Electrical Engineering at Beihang University. She received her Ph.D. degree from Northwestern Polytechnical University. Her current research interests are guidance and control, fault detection and isolation, and healthy management.